Taken together, our findings demonstrate that miR-140 is required for skeletal development and cartilage homeostasis, and protects against OA-like pathology via *Adamts-5* regulation (Fig. 7). We conclude that miR-140 is a novel regulator of cartilage homeostasis, and changes in its expression and function play an important role in diseases associated with cartilage destruction, including OA and inflammatory arthropathies.

Materials and methods

Generation of miR-140-null mice and miR-140 TG mice

All animal experiments were performed according to protocols approved by the Institutional Animal Care and Use Committee at The Scripps Research Institute and National Institute for Child Health and Development. A vector was constructed to replace the endogenous miR-140 locus with a PGK-neo cassette by homologous recombination in embryonic stem (ES) cells. The 5′ and 3′ sequences flanking the endogenous miR-140 locus were amplified by PCR from a C57BL/6 genomic BAC clone (BACPAC Resource Center). These homologous arms were cloned into a vector incorporating both a neomycin resistance cassette for positive selection and a diphtheria toxin (DTA) gene for negative selection. The targeting vector was linearized and electroporated into TT2F mouse ES cells. Recombinant ES clones were isolated after culture in medium containing G418 antibiotic. Clones were then screened for proper integration by Southern blot analysis with the 5′ probe, 3′ probe, and neomycin resistance cassette sequence indicated in Figure 1. After proper integration was validated by genomic sequencing, two clones were chosen for microinjection into eight-cell-stage embryos. The resulting chimeric offspring were crossed with C57BL/6 mice, and germline transmission was confirmed by Southern blot and PCR. The floxed PGK-neo cassette was removed by crossing with Meox-Cre TG mice; Cre-mediated neo excision was confirmed by genomic PCR.

To generate cartilage-specific miR-140 TG mice, a pri-miR-140 fragment was PCR-amplified from mouse chondrocyte cDNA with the primers 5′-TGGTGTGTGGTTCTATGCCAGC-3′ and 5′-AG CCTCAAGCCAGAATTCAGG-3′.

pri-miR-140 was cloned into the NotI site of a Col2a1-based expression vector (Ueta et al. 2001), which contained the promoter and enhancer of the mouse Col2a1 gene. TG mice were generated by pronuclear injection of the transgene into the B6 strain, and were backcrossed to a C57BL/6 background. Genomic DNA isolated from the tail was analyzed by PCR using specific primers or transgene probes (forward primer, 5′-CAGGCTGTGC TTGGTGGGCATCTG-3′; reverse primer, 5′-CTAGCCTAGGC TCGAGAAGCTTGCT-3′).

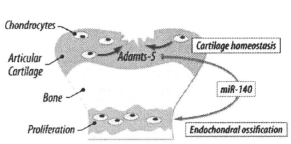

Figure 7. *Adamts-5* regulation via miR-140 is required for skeletal development and cartilage homeostasis. miR-140 has dual roles in both endochondral ossification and articular cartilage homeostasis. During endochondral ossification, miR-140 is important for chondrocyte proliferation, although its targets are unclear. miR-140 also plays a critical role in articular cartilage homeostasis by repressing *Adamts-5* expression.

qPCR

qPCR was performed using TaqMan Gene Expression Assay probes for *Adamts-5* (Mm01344182_m1) and glyceraldehyde 3-phosphate dehydrogenase (*GAPDH*; Mm 99999915_g1; Applied Biosystems), and qPCR for miR-140 was performed using the TaqMan MicroRNA Reverse Transcription kit (Applied Biosystems) according to the manufacturer's protocol. *GAPDH* or sno202 was used as an internal control to normalize sample differences.

Western blot analysis

Total protein extracts of wild-type and miR-140$^{-/-}$ chondrocytes were prepared for Western blot analysis. The Wwp2 protein, which is encoded by the host gene of miR-140, was detected by the AIP2 antibody (dilution, 1:2000; sc-11896, Santa Cruz Biotechnologies).

Radiologic imaging

X-ray and micro-CT imaging were performed using LaTheta LCT-200 (Aloka) according to the manufacturer's instructions. Three-dimensional CT images of the knee joint were recreated by using VGStudio MAX 2.0 software (Nihon Visual Science).

Bromodeoxyuridine (BrdU) labeling, RNA in situ hybridization, and immunohistochemistry

Proliferating cells were detected by BrdU incorporation using the In Situ Cell Proliferation kit, FLUOS (Roche); 4′,6-diamidino-2-phenylindole (DAPI) served as a counterstain. In situ hybridization of miR-140 was performed as described previously (Yokoyama et al. 2009). We used a probe specific for the primary region of miR-140. The sections of knee joints were immunostained using antibodies against ADAMTS-5 (ab13976, Abcam) and type II collagen (II-II6B3, Hybridoma Bank).

Histopathologic assessment

The miR-140$^{-/-}$ mice and wild-type littermates were obtained from the intercross of miR-140$^{+/-}$ maintained in a C57BL/6 background. Whole-mount Alcian blue and Alizarin red S staining of skeletons were performed on wild-type and miR-140$^{-/-}$ embryos at embryonic day 17.5 (E17.5). Mice were euthanized, and knee joints were harvested from 3-, 8-, and 12-mo-old mice. The knee joints were fixed in 10% zinc-buffered formalin (Z-Fix; Anatech) and decalcified in decalcifier (TBD-2; Shandon). For each animal, 4-μm sagittal sections through the central weight-bearing region of the medial femorotibial joint were stained with Safranin O and Fast Green for analysis of histopathologic differences between wild-type and miR-140$^{-/-}$ mice. The proteoglycan content of articular cartilage was scored using the previously reported Mankin scoring system (Mankin 1971; Zemmyo et al. 2003). OA scores indicating the severity of cartilage degeneration were evaluated for wild-type (n = 6) and miR-140$^{-/-}$ (n = 6) 3-mo-old mice, wild-type (n = 15) and miR-140$^{-/-}$ (n = 13) 8-mo-old mice, and wild-type (n = 12) and miR-140$^{-/-}$ (n = 11) 12-mo-old mice. At least four sections per sample were analyzed microscopically and scored using previously reported semiquantitative scoring systems (Chambers et al. 2001; Glasson et al. 2004).

Mouse model of surgically induced OA

Surgical OA was induced in wild-type and miR-140$^{-/-}$ mice at the age of 10 wk by resecting the MMTL in the right knee joint (Glasson et al. 2007). Pathological changes in medial tibial plateau and medial femoral condyle of the joint were evaluated after 8 wk on safranin-O-stained sections by OA score.

Mouse model of AIA

Inflammatory arthritis was induced in knee joints of 10-wk-old wild-type (n = 5), miR-140$^{-/-}$ (n = 6), and miR-140 TG (n = 6) mice by intra-articular injection of methylated bovine serum albumin (mBSA; Sigma catalog no. A1009) in mice preimmunized with mBSA. On day 1, mice were preimmunized by a 100-μL intradermal injection at the base of the tail with an emulsion containing 100 μg of mBSA (in 0.9% saline) and an equal volume of Freund's complete adjuvant (Sigma catalog no. F5881). On day 10, animals were treated with intra-articular mBSA (10 μL of 20 mg/mL mBSA in 0.9% sterile saline or vehicle alone) into the left and right knee joints. On day 17, the knee joints were harvested and processed using standard procedures.

DNA microarray analysis

DNA microarray analysis was performed using the Affymetrix mouse genome 430 2.0 array. RNA samples were collected from cultured rib chondrocytes of wild-type and miR-140$^{-/-}$ mice at P3. Microarray data were summarized by the Robust Multichip Average (RMA) method, and statistical analysis was performed using National Institute on Aging (NIA) Array Analysis (http://Igsun.grc.nia.nih.gov/ANOVA). The microarray data were deposited in the Gene Expression Omnibus (GEO) repository under accession number GSE16007.

Bioinformatics and miR-140 target analysis

We performed searches on the TargetScan prediction program (http://targetscan.org) for the predicted targets of miR-140.

Quantification of proteoglycan

Femoral heads were harvested from 4-wk-old wild-type and miR-140$^{-/-}$ mice. The explants were cultured for 3 d with or without IL-1β (5 ng/mL) in Dulbecco's modified Eagle's medium (DMEM) containing 10 mM HEPES and 1% penicillin/streptomycin. At the end of the culture, the cartilage explants were digested with protease K solution (Tris-EDTA at pH 8.0, 30 μg/mL protease K, 0.5% Tween 20) overnight at 50°C. Proteoglycan content in the protease K digests and conditioned medium were determined using the Blyscan Glycosaminoglycan Assay kit (Biocolor).

Cell culture and transfection of ds-miR-140 assay

Mouse chondrocytes were prepared from rib cartilage of P3 mice by digestion with collagenase. Mouse chondrocytes were cultured in DMEM with 10% fetal bovine serum (FBS) at 37°C. dsRNA oligonucleotides (5 nM) representing mature sequences that mimic endogenous miR-140 and Silencer Negative Control siRNA #1 (Ambion) were transfected into chondrocytes with Lipofectamine 2000 (Invitrogen). The synthesized RNA oligonucleotides 5′-CAGUGGUUUUACCCUAUGGUAG-3′ and 5′-ACCACAGGGUAGAACCACGGAC-3′ were annealed to obtain ds-miR-140. Silencer Negative Control siRNA #1 (siNega) was used at the same concentration as the specific miR-140 ds RNA in each experiment.

Luciferase assay

To create the pLuc2 reporter vector, a luciferase 2 gene (Promega) was incorporated into a modified pGL3-control plasmid with HindIII and EcoRI. To create the pGL3-miR-140 sensor vector (miR-140 sensor), the following chemically synthesized miR-140 multiple target sites were annealed and inserted between EcoRI and XhoI sites downstream from the firefly luciferase coding region in a pGL3 luciferase reporter plasmid with a modified 3′ UTR sequence (sense strand, 5′-AATTCTACCATAGGGTAAAACCACTGCTACCATAGGGTAAAACCACTGCTACCATAGGGTAAAACCACTG-3′; antisense strand, 5′-TCGACAGTGGTTTTACCCTATGGTAGCAGTGGTTTTACCCTATGGTAGCAGTGGTTTTACCCTATGGTAGCAGTGGTTTTACCCTATGG-3′). To create the pLuc2-*Adamts-5* 3′ UTR vector (*Adamts-5* 3′ UTR), a fragment of the 3′ UTR of *Adamts-5* gene including the predicted miR-140-binding site was PCR-amplified using the primer set 5′-TGAATTCCTACTCTGCTTCCCTCTATGATC-3′ and 5′-TTCTCGAGCTGTGTTTCTTTCCTCAGGAG-3′, and then cloned downstream from the luciferase 2 gene with EcoRI and XhoI. To create the reporter vector with mutated miR-140-binding site (*Adamts-5* mut 3′ UTR), the 3′ UTR of *Adamts-5* was amplified with the primer set 5′-TGAATTCCTACTCTGCTTCCCTCTATGATC-3′ and 5′-CCCTCTAGACATAGATTTGACGAATATCCGTTTACCCTCCTTAGG-3′, and then cloned into a *Adamts5* 3′ UTR-containing vector with EcoRI and XbaI. ds-miR-140 and the scrambled siRNA sequences (AGUUGCACGCGCAAUUAdCdC and UAAUUGCGCGUGCAACUdTdT; final concentration, 50 nM) were reverse-transfected with Lipofectamine RNAiMAX (Invitrogen) into HEK293T cells (2.0×10^4 cells per well in a 96-well plate). After 24 h of transfection, culture medium was changed, and the firefly luciferase reporter plasmid (20 ng) and Renilla luciferase control plasmid pRL-SV40 (20 ng) were transfected with Lipofectamine 2000 (Invitrogen). Luciferase activity was determined with the Dual-Glo Luciferase Assay System (Promega).

Statistical analysis

Two-tailed independent Student's t-test and the nonparametric Wilcoxon signed-rank test were used for statistical analysis. Asterisks indicate differences with statistical significance at $P < 0.05$ (*) and $P < 0.01$ (**).

Acknowledgments

We thank E. Kim for her excellent technical support, and extend our gratitude to all other members in the laboratory. We also thank Y. Takahashi and M. Asada for their bioinformatics assistance, and E. Lamar for critical reading of the manuscript and discussion. T.S. and H.A. are associate scientists of Tokyo Medical and Dental University. This project was supported by NIH AR050631 (to H.A.), AR056120 (to H.A.), AG007996 (to M.K.L.), and AG033409 (to M.K.L.); the Arthritis National Research Foundation (S.M.); the Arthritis Foundation (S.O.); grants from the Ministry of Health, Labour, and Welfare; the Genome Network Project (MEXT); grants-in-aid for Scientific Research (MEXT); and grants from National Institute of Biomedical Innovation, Research on Child Health and Development, and The Japan Health Sciences Foundation.

References

Akiyama H. 2008. Control of chondrogenesis by the transcription factor Sox9. *Mod Rheumatol* **18:** 213–219.

Bartel DP. 2004. MicroRNAs: Genomics, biogenesis, mechanism, and function. *Cell* **116:** 281–297.

Chambers MG, Cox L, Chong L, Suri N, Cover P, Bayliss MT, Mason RM. 2001. Matrix metalloproteinases and aggrecanases cleave aggrecan in different zones of normal cartilage but colocalize in the development of osteoarthritic lesions in STR/ort mice. *Arthritis Rheum* **44:** 1455–1465.

de Crombrugghe B, Lefebvre V, Behringer RR, Bi W, Murakami S, Huang W. 2000. Transcriptional mechanism of chondrocyte differentiation. *Matrix Biol* **19:** 389–394.

Elia L, Quintavalle M, Zhang J, Contu R, Cossu L, Latronico MV, Peterson KL, Indolfi C, Catalucci D, Chen J, et al. 2009. The knockout of miR-143 and -145 alters smooth muscle cell maintenance and vascular homeostasis in mice: Correlates with human disease. *Cell Death Differ* **16:** 1590–1598.

Glasson SS, Askew R, Sheppard B, Carito BA, Blanchet T, Ma HL, Flannery CR, Kanki K, Wang E, Peluso D, et al. 2004. Characterization of and osteoarthritis susceptibility in ADAMTS-4-knockout mice. *Arthritis Rheum* **50:** 2547–2558.

Glasson SS, Askew R, Sheppard B, Carito B, Blanchet T, Ma HL, Flannery CR, Peluso D, Kanki K, Yang Z, et al. 2005. Deletion of active ADAMTS5 prevents cartilage degradation in a murine model of osteoarthritis. *Nature* **434:** 644–648.

Glasson SS, Blanchet TJ, Morris EA. 2007. The surgical destabilization of the medial meniscus (DMM) model of osteoarthritis in the 129/SvEv mouse. *Osteoarthritis Cartilage* **15:** 1061–1069.

Goldring MB, Goldring SR. 2007. Osteoarthritis. *J Cell Physiol* **213:** 626–634.

Goldring MB, Marcu KB. 2009. Cartilage homeostasis in health and rheumatic diseases. *Arthritis Res Ther* **11:** 224. doi: 10.1186/ar2592.

Harfe BD, McManus MT, Mansfield JH, Hornstein E, Tabin CJ. 2005. The RNaseIII enzyme Dicer is required for morphogenesis but not patterning of the vertebrate limb. *Proc Natl Acad Sci* **102:** 10898–10903.

Hashimoto M, Nakasa T, Hikata T, Asahara H. 2008. Molecular network of cartilage homeostasis and osteoarthritis. *Med Res Rev* **28:** 464–481.

Iliopoulos D, Malizos KN, Oikonomou P, Tsezou A. 2008. Integrative microRNA and proteomic approaches identify novel osteoarthritis genes and their collaborative metabolic and inflammatory networks. *PLoS One* **3:** e3740. doi: 10.1371/journal.pone.0003740.

Kobayashi T, Lu J, Cobb BS, Rodda SJ, McMahon AP, Schipani E, Merkenschlager M, Kronenberg HM. 2008. Dicer-dependent pathways regulate chondrocyte proliferation and differentiation. *Proc Natl Acad Sci* **105:** 1949–1954.

Krebsbach PH, Nakata K, Bernier SM, Hatano O, Miyashita T, Rhodes CS, Yamada Y. 1996. Identification of a minimum enhancer sequence for the type II collagen gene reveals several core sequence motifs in common with the link protein gene. *J Biol Chem* **271:** 4298–4303.

Lewis BP, Burge CB, Bartel DP. 2005. Conserved seed pairing, often flanked by adenosines, indicates that thousands of human genes are microRNA targets. *Cell* **120:** 15–20.

Lim LP, Lau NC, Garrett-Engele P, Grimson A, Schelter JM, Castle J, Bartel DP, Linsley PS, Johnson JM. 2005. Microarray analysis shows that some microRNAs downregulate large numbers of target mRNAs. *Nature* **433:** 769–773.

Lin AC, Seeto BL, Bartoszko JM, Khoury MA, Whetstone H, Ho L, Hsu C, Ali AS, Alman BA. 2009. Modulating hedgehog signaling can attenuate the severity of osteoarthritis. *Nat Med* **15:** 1421–1425.

Liu N, Bezprozvannaya S, Williams AH, Qi X, Richardson JA, Bassel-Duby R, Olson EN. 2008. microRNA-133a regulates cardiomyocyte proliferation and suppresses smooth muscle gene expression in the heart. *Genes Dev* **22:** 3242–3254.

Malfait AM, Liu RQ, Ijiri K, Komiya S, Tortorella MD. 2002. Inhibition of ADAM-TS4 and ADAM-TS5 prevents aggrecan degradation in osteoarthritic cartilage. *J Biol Chem* **277:** 22201–22208.

Mankin HJ. 1971. Biochemical and metabolic aspects of osteoarthritis. *Orthop Clin North Am* **2:** 19–31.

Miyaki S, Nakasa T, Otsuki S, Grogan SP, Higashiyama R, Inoue A, Kato Y, Sato T, Lotz MK, Asahara H. 2009. MicroRNA-140 is expressed in differentiated human articular chondrocytes and modulates interleukin-1 responses. *Arthritis Rheum* **60:** 2723–2730.

Nakasa T, Miyaki S, Okubo A, Hashimoto M, Nishida K, Ochi M, Asahara H. 2008. Expression of microRNA-146 in rheumatoid arthritis synovial tissue. *Arthritis Rheum* **58:** 1284–1292.

Stanczyk J, Pedrioli DM, Brentano F, Sanchez-Pernaute O, Kolling C, Gay RE, Detmar M, Gay S, Kyburz D. 2008. Altered expression of microRNA in synovial fibroblasts and synovial tissue in rheumatoid arthritis. *Arthritis Rheum* **58:** 1001–1009.

Stanton H, Rogerson FM, East CJ, Golub SB, Lawlor KE, Meeker CT, Little CB, Last K, Farmer PJ, Campbell IK, et al. 2005. ADAMTS5 is the major aggrecanase in mouse cartilage in vivo and in vitro. *Nature* **434:** 648–652.

Stefani G, Slack FJ. 2008. Small non-coding RNAs in animal development. *Nat Rev Mol Cell Biol* **9:** 219–230.

Thirunavukkarasu K, Pei Y, Wei T. 2007. Characterization of the human ADAMTS-5 (aggrecanase-2) gene promoter. *Mol Biol Rep* **34:** 225–231.

Tuddenham L, Wheeler G, Ntounia-Fousara S, Waters J, Hajihosseini MK, Clark I, Dalmay T. 2006. The cartilage specific microRNA-140 targets histone deacetylase 4 in mouse cells. *FEBS Lett* **580:** 4214–4217.

Ueta C, Iwamoto M, Kanatani N, Yoshida C, Liu Y, Enomoto-Iwamoto M, Ohmori T, Enomoto H, Nakata K, Takada K, et al. 2001. Skeletal malformations caused by overexpression of Cbfa1 or its dominant negative form in chondrocytes. *J Cell Biol* **153:** 87–100.

Valencia-Sanchez MA, Liu J, Hannon GJ, Parker R. 2006. Control of translation and mRNA degradation by miRNAs and siRNAs. *Genes Dev* **20:** 515–524.

van Rooij E, Sutherland LB, Liu N, Williams AH, McAnally J, Gerard RD, Richardson JA, Olson EN. 2006. A signature pattern of stress-responsive microRNAs that can evoke cardiac hypertrophy and heart failure. *Proc Natl Acad Sci* **103:** 18255–18260.

van Rooij E, Sutherland LB, Qi X, Richardson JA, Hill J, Olson EN. 2007. Control of stress-dependent cardiac growth and gene expression by a microRNA. *Science* **316:** 575–579.

Vega RB, Matsuda K, Oh J, Barbosa AC, Yang X, Meadows E, McAnally J, Pomajzl C, Shelton JM, Richardson JA, et al. 2004. Histone deacetylase 4 controls chondrocyte hypertrophy during skeletogenesis. *Cell* **119:** 555–566.

Wienholds E, Kloosterman WP, Miska E, Alvarez-Saavedra E, Berezikov E, de Bruijn E, Horvitz HR, Kauppinen S, Plasterk RH. 2005. MicroRNA expression in zebrafish embryonic development. *Science* **309:** 310–311.

Xiao C, Rajewsky K. 2009. MicroRNA control in the immune system: Basic principles. *Cell* **136:** 26–36.

Yamasaki K, Nakasa T, Miyaki S, Ishikawa M, Deie M, Adachi N, Yasunaga Y, Asahara H, Ochi M. 2009. Expression of microRNA-146a in osteoarthritis cartilage. *Arthritis Rheum* **60:** 1035–1041.

Yokoyama S, Ito Y, Ueno-Kudoh H, Shimizu H, Uchibe K, Albini S, Mitsuoka K, Miyaki S, Kiso M, Nagai A., et al. 2009. A systems approach reveals that the myogenesis genome

network is regulated by the transcriptional repressor RP58. *Dev Cell* **17:** 836–848.

Zemmyo M, Meharra EJ, Kuhn K, Creighton-Achermann L, Lotz M. 2003. Accelerated, aging-dependent development of osteoarthritis in α1 integrin-deficient mice. *Arthritis Rheum* **48:** 2873–2880.

Zhao Y, Ransom JF, Li A, Vedantham V, von Drehle M, Muth AN, Tsuchihashi T, McManus MT, Schwartz RJ, Srivastava D. 2007. Dysregulation of cardiogenesis, cardiac conduction, and cell cycle in mice lacking miRNA-1-2. *Cell* **129:** 303–317.

Zhou G, Garofalo S, Mukhopadhyay K, Lefebvre V, Smith CN, Eberspaecher H, de Crombrugghe B. 1995. A 182 bp fragment of the mouse pro α 1(II) collagen gene is sufficient to direct chondrocyte expression in transgenic mice. *J Cell Sci* **108:** 3677–3684.

The *Mohawk* homeobox gene is a critical regulator of tendon differentiation

Yoshiaki Ito[a], Naoya Toriuchi[a], Teruhito Yoshitaka[a], Hiroe Ueno-Kudoh[a], Tempei Sato[a], Shigetoshi Yokoyama[a], Keiichiro Nishida[b], Takayuki Akimoto[c], Michiko Takahashi[a], Shigeru Miyaki[a], and Hiroshi Asahara[a,1]

[a]Department of Systems BioMedicine, National Research Institute for Child Health and Development, Tokyo 157-8535, Japan; [b]Department of Human Morphology, Science of Functional Recovery and Reconstruction, Okayama University Graduate School of Medicine and Dentistry, Okayama 700-8558, Japan; and [c]Laboratory of Regenerative Medical Engineering, Center for Disease Biology and Integrative Medicine, Graduate School of Medicine, University of Tokyo, Tokyo 113-0033, Japan

Edited* by Marc R. Montminy, The Salk Institute for Biological Studies, La Jolla, CA, and approved May 5, 2010 (received for review January 20, 2010)

***Mohawk* (*Mkx*) is a member of the Three Amino acid Loop Extension superclass of atypical homeobox genes that is expressed in developing tendons. To investigate the in vivo functions of Mkx, we generated *Mkx*$^{-/-}$ mice. These mice had hypoplastic tendons throughout the body. Despite the reduction in tendon mass, the cell number in tail tendon fiber bundles was similar between wild-type and *Mkx*$^{-/-}$ mice. We also observed small collagen fibril diameters and a down-regulation of type I collagen in *Mkx*$^{-/-}$ tendons. These data indicate that Mkx plays a critical role in tendon differentiation by regulating type I collagen production in tendon cells.**

Tendons are dense, fibrous connective tissues that connect muscle to bone, transmitting the forces that allow for body movement (1). Tendon damage from overuse or degeneration due to aging is a common clinical problem because damaged tendon tissue heals very slowly and rarely recovers completely (2). The establishment of new therapies, such as regenerative medicine, for injured tendons has been delayed by a limited understanding of tendon biology (1, 3).

Tendons are composed primarily of collagen fibrils that cross-link to each other to form fibers (4). A small number of tendon cells reside between parallel chains of these fibrils and synthesize the specific ECM that contains collagens and proteoglycans (4, 5). The elasticity of tendons is provided by the large amount of collagen, predominantly type I collagen and small amounts of other collagens, including types III, IV, V, and VI (4, 6–9). The proteoglycans found in tendons, including decorin, fibromodulin, biglycan, and lumican, act to lubricate and organize collagen fiber bundles (4, 5). Targeted disruption of these proteoglycans in mice leads to abnormal collagen fibrils in tendons (3, 10–13). Tendon disruptions have also been described in patients with defects in collagen production, such as Ehlers-Danlos Syndrome, in which the type I collagen gene is mutated (14). These studies indicate that the ability of tendon cells to produce ECM is important for tendon formation.

Recently, it was reported that *Scleraxis* (*Scx*), a basic helix–loop–helix (bHLH) transcription factor expressed in the tendon progenitors and cells of all tendon tissues (15, 16), is essential for tendon differentiation. *Scx* knockout mice show severe disruption of force-transmitting tendons, although ligaments, which are tissues connecting bone to bone that closely resemble tendons in their components, and short-range anchoring tendons are not affected (17). It was also reported that Scx positively regulates the expression of type I collagen, a main ECM component of tendons (18). However, the type I collagen does not completely disappear from the tendons of *Scx* knockout mice (17), suggesting the presence of other regulatory factors for type I collagen. The tendon differentiation mechanisms remain largely unknown, with Scx being the only known transcription factor regulating tendon differentiation.

Mohawk (*Mkx*; also known as *Irxl1*) is the sole member of a newly characterized class within the Three Amino acid Loop Extension (TALE) superclass of atypical homeobox genes (19). These transcription factors are essential for a large set of developmental processes, including cell proliferation, differentiation, and positional specification (20–24). Initial characterization of mouse *Mkx* revealed a dynamic transcription pattern restricted to progenitors of tendon, skeletal muscle, and cartilage, as well as the sex chords of the male gonad and the ureteric bud tip of the metanephrogenic kidney (19, 25, 26). We previously identified *Mkx* as a transcription factor expressed in developing tendons by constructing a whole-mount in situ hybridization database, termed "EMBRYS" (http://embrys.jp/embrys/html/MainMenu.html), which contains expression data of 1,520 transcription factors and cofactors expressed in E9.5, E10.5, and E11.5 mouse embryos (27).

To investigate the in vivo functions of Mkx, we generated *Mkx* knockout mice. Here, we show that *Mkx* null mice have hypoplastic tendons throughout their body. Although the size of tendons is drastically reduced in *Mkx* null mice, the cell number in tail tendon fiber bundles shows no significant difference between wild-type and *Mkx* null mice. We also observed abnormal collagen fibrils in *Mkx* null tendons. Furthermore, we show that the expression of type I collagen, which is a major tendon ECM component, is down-regulated in the Achilles tendon of *Mkx* null mice. These data indicate that Mkx is a transcription factor controlling tendon differentiation by regulating type I collagen production in tendon cells.

Results

Generation of *Mkx* Mutant Mice. We inactivated the *Mkx* gene by homologous recombination in ES cells using a targeting vector to replace the *Mkx* gene from the start of translation to the end of exon 2 with the Venus gene and PGK-neomycin-resistance (PGK-neo) cassette (Fig. 1*A*). We predicted that the Venus gene, an improved GFP gene (28), would be expressed in *Mkx* positive cells in heterozygous mice generated with the targeting construct. We identified two correctly targeted ES cell clones by Southern blot analysis (Fig. S1 *A* and *B*). These two clones were microinjected into 8-cell stage embryos and germ-line transmission in the resulting chimeric mice was confirmed by Southern blotting and genomic PCR (Fig. 1*B* and Fig. S1*C*). *Mkx*$^{+/-}$ embryos showed robust Venus expression that recapitulated *Mkx* expression faithfully at E13.5 forelimb and tail (Fig. 1*C*). Also, these *Venus* knockin heterozygous mice showed tendon-specific Venus expression in the tail of E16.5 embryos (Fig. 1*D*). In addition to embryos, we investigated Venus expression in adult mice. Because Mkx expression in tendons of adult mice had not been determined, we analyzed

Author contributions: Y.I., S.Y., and H.A. designed research; Y.I., N.T., T.Y., H.U.-K., T.S., S.Y., K.N., T.A., M.T., and H.A. performed research; Y.I., H.U.-K., T.S., and H.A. contributed new reagents/analytic tools; Y.I., N.T., T.Y., S.Y., K.N., T.A., S.M., and H.A. analyzed data; and Y.I. and H.A. wrote the paper.

The authors declare no conflict of interest.

*This Direct Submission article had a prearranged editor.

Freely available online through the PNAS open access option.

[1]To whom correspondence should be addressed. E-mail: asahara@nch.go.jp.

This article contains supporting information online at www.pnas.org/lookup/suppl/doi:10.1073/pnas.1000525107/-/DCSupplemental.

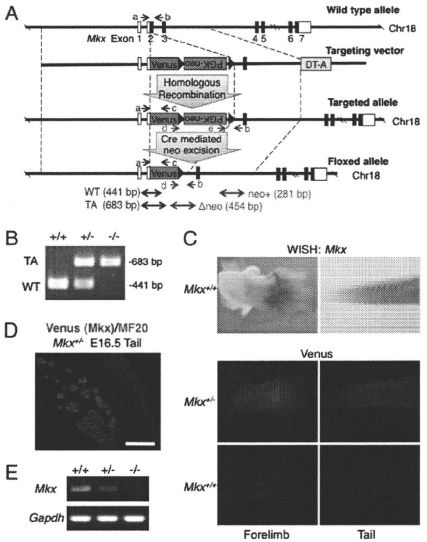

Fig. 1. Generation of *Mkx* mutant mice. (*A*) Diagram of the *Mkx* targeting construct. Blue and red arrows (*a–e*) show genomic PCR primers for genotyping. White box, UTR; Black box, coding region; DT-A, diphtheria toxin A; WT, wild-type allele; TA, targeted allele. (*B*) Genomic PCR of wild-type and *Mkx* mutant mice for genotyping using primers a, b and c. (*C*) Whole-mount in situ hybridization of *Mkx* (*Upper*) and whole-mount visualization of Venus signals (*Lower*) in E13.5 forelimb and tail of wild-type or *Mkx* mutant embryos. (*D*) Immunohistochemistry for anti-myosin heavy chain (MF20; red) and visualization of Venus in cryosection of E16.5 tail of a Venus knockin *Mkx* heterozygous embryo. (Scale bar, 100 μm.) (*E*) RT-PCR analysis for *Mkx* and *Gapdh* of Achilles tendon in wild-type and *Mkx* mutant mice.

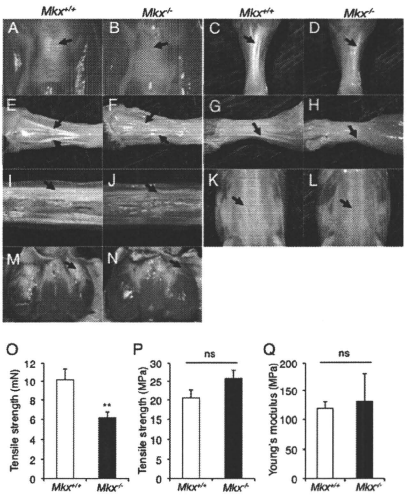

Fig. 2. Tendon defects are observed in *Mkx* null mice. (*A–N*) The appearance of the patellar tendon (*A* and *B*; black arrow), Achilles tendon (*C* and *D*; black arrow), hindlimb tendons (*E* and *F*), forelimb tendons (*G* and *H*), tail tendons (*I* and *J*), back tendons (*K* and *L*; black arrow) and platysma tendon (*M* and *N*; black arrow) in 3-month-old wild-type and *Mkx* null mice. (*O* and *P*) Absolute value of tensile strength (*O*) and tensile strength per unit area (*P*) of Achilles tendons in wild-type and *Mkx* null mice. Error bars, SEM ($n = 7$). ns, no significance. (*Q*) Young's modulus of Achilles tendons in wild-type and *Mkx* null mice. Error bars, SEM ($n = 7$). ns, no significance.

expression of *Mkx* in tendon tissues of C57BL/6 adult mice by RT-PCR and found that *Mkx* was strongly expressed (Fig. S2*A*). Venus was specifically expressed in Achilles, tail, and trunk tendons of 6-week-old *Mkx* heterozygous mice (Fig. S2 *B–M*). These data indicate that this mutant mouse is useful for tendon biological analysis and expression analysis of *Mkx*. To confirm inactivation of the *Mkx* gene, we performed RT-PCR analysis of *Mkx* mutant mice. The analysis of adult Achilles tendon RNA showed a complete absence of *Mkx* expression in $Mkx^{-/-}$ mice (Fig. 1*E*). Genotyping of 206 newborn offspring derived from heterozygous–heterozygous crosses revealed a normal Mendelian ratio of genotypes (Table S1). Heterozygous and homozygous mutant mice were viable and fertile, and weight measurements did not show differences compared with wild-type mice (Fig. S3).

Tendon Defects Are Observed in *Mkx* Null Mice. To investigate the function of *Mkx* in tendon formation, we analyzed tendons of *Mkx* null mice. Tendons (patellar, Achilles, and tail tendons, dorsal extensor tendons of the forelimb and hindlimb, tendons of the trunk, and platysma tendons) of 3-month-old *Mkx* null mice were hypoplastic and pale white in color compared with those of wild-type mice (Fig. 2 *A–N*). This phenotype was also observed in *Mkx* null mice, in which a neo cassette was excised by Cre recombination (Fig. S4); however, heterozygous mice with or without a neo cassette were not affected (Fig. S2 *B–M*). To examine the mechanical properties of *Mkx* null tendons, we performed a tensile test. These experiments showed a diminution of tensile strength in *Mkx* null Achilles tendons (Fig. 2*O*), indicating functional depression. However, tensile strength per unit area and Young's modulus, which is a measure of the stiffness of an isotropic elastic material indicating elasticity per unit area, did not show significant change between wild-type and *Mkx* null mice (Fig. 2 *P* and *Q*). This suggests that the diminution of tensile strength in *Mkx* null tendons is due to reduced tendon mass.

We performed histological analyses to further confirm the tendon defects observed in *Mkx* null mice. H&E staining of patellar tendons from 3-month-old *Mkx* null mice revealed that *Mkx* null patellar tendons were thinner than wild-type tendons (Fig. 3*A a–d*). Seven-day-old *Mkx* null mice also had thin patellar tendons, which were approximately half the thickness of the tendons from wild-type mice (Fig. 3*B*). However, the cruciate ligament, which closely resembles tendons with regard to its components, was not affected in *Mkx* knockout mice (Fig. S5). Tail tendons in *Mkx* null mice also show small tendon fiber bundles (Fig. 3*A e–h*; yellow arrowheads). However, *Mkx* null tail tendons had high tendon cell density and the cell number of tail tendon fiber bundles was not significantly different between wild-type and *Mkx* null mice (Fig. 3*C*). The enhanced cell density was also observed in the Achilles tendon of knockout mice (Fig. 3*C*). This suggests that *Mkx* null tendon cells are not completely functional.

To determine whether tendon defects in *Mkx* knockout mice are also observed in embryonic stages, we performed azan staining of tail tendons in *Mkx* null embryos at E18.5. The size of the tail

DEVELOPMENTAL BIOLOGY

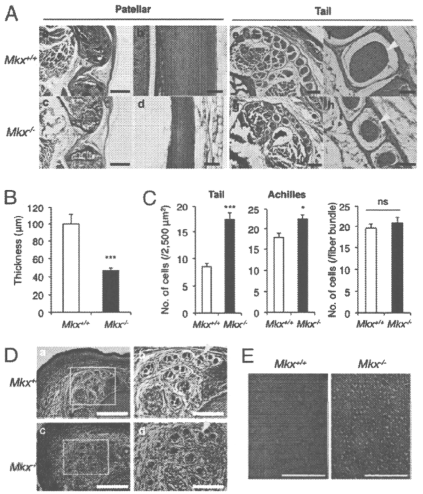

Fig. 3. Tendon mass is decreased in *Mkx* null mice. (*A*) H&E staining of the patellar (*a–d*) and tail (*e–h*) tendons in 3-month-old wild-type and *Mkx* null mice. Yellow arrowheads indicate a fiber bundle in the tail tendon. [Scale bars: (*a* and *c*) 1 mm; (*b* and *d*) 50 μm; (*e* and *g*) 200 μm; (*f* and *h*) 50 μm.] (*B*) Patellar tendon thickness of 7-day-old wild-type and *Mkx* null mice. Error bars, SEM (n = 8). (*C*) Cell density of tail or Achilles tendons (*Left*) and cell number in a tail tendon fiber bundle (*Right*) in 3-month-old wild-type and *Mkx* null mice. Error bars, SEM (*Left*, n = 8 ~10; *Right*, n = 14). ns, no significance. (*D*) Azan staining of E18.5 embryonic tails in wild-type and *Mkx* null mice. Yellow arrowheads indicate a fiber bundle in the tail tendon. [Scale bars: (*Left*) 500 μm; (*Right*) 200 μm.] (*E*) Transmission electron microscopic view of collagen fibrils in the Achilles tendon of wild-type and *Mkx* null mice. (Scale bars, 200 nm.)

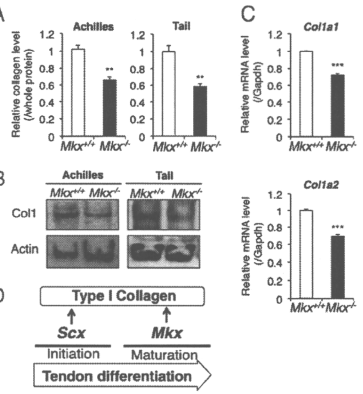

Fig. 4. Type I collagen productivity is decreased in *Mkx* null tendon cells. (*A*) Soluble collagen measurement in whole soluble protein of Achilles or tail tendons of 8-week-old wild-type or *Mkx* null mice. Error bars, SEM (n = 3). (*B*) Western blot analysis of type I collagen (Col1) and β-actin (actin) in Achilles or tail tendons of 8-week-old wild-type or *Mkx* null mice. (*C*) Real-time PCR analysis for *Col1a1* and *Col1a2* in Achilles tendons of 8-week-old wild-type or *Mkx* null mice. Error bars, SEM (n = 3). (*D*) Proposed tendon differentiation network.

tendons in *Mkx* null embryos was not affected, but we observed a low density of aniline blue staining (Fig. 3*D*; yellow arrowheads), which detects collagen fibers. To analyze the collagen fibrils of *Mkx* null tendons in detail, we performed an ultrastructural analysis of Achilles tendons using electron microscopy. Collagen fibril diameters in the *Mkx* null mice were uniformly smaller than those of wild-type mice (Fig. 3*E*). These data suggest a reduction of collagens in *Mkx* null tendons and a critical role for *Mkx* in tendon differentiation in vivo.

***Mkx* Null Tendon Cells Reduced Type I Collagen Production.** Despite tendon mass reduction in *Mkx* null mice, tendon cell number showed no significant changes between wild-type and *Mkx* null mice (Fig. 3*C*). This suggests that *Mkx* null tendon cells have a reduced ability to synthesize ECM or enhance ECM catabolic activity. In addition, histological analysis by azan staining of E18.5 *Mkx* null tail tendons (Fig. 3*D*) and ultrastructural analysis of Achilles tendons (Fig. 3*E*) suggested a reduction of collagens in *Mkx* null tendons. To investigate the production of collagens by *Mkx* null tendon cells, we first measured the amount of soluble collagens in *Mkx* null tendons by Sircol Soluble Collagen Assay. This experiment indicated that total soluble collagens were decreased in Achilles and tail tendons of *Mkx* null mice compared with those from wild-type mice (Fig. 4*A*). Furthermore, we found a reduction in the protein level of type I collagen, which is a main component of tendon ECM, in Achilles and tail tendons of *Mkx* knockout mice by Western blotting (Fig. 4*B*). We also found that the mRNA levels of *Col1a1* and *Col1a2*, which encode the type I collagen, were decreased in Achilles tendons of *Mkx* null mice through quantitative real-time PCR (Fig. 4*C*). However, the expression of the transcription factor *Scx*, which is a positive regulator of type I collagen, was not reduced and rather increased in these tendons (Fig. S6), indicating that the decrease of collagen I is not due to the down-regulation of *Scx*. We also investigated the expression of other tendon component genes such as *elastin* (*Eln*), *fibrillin1* (*Fbn1*), *Col3a1*, *Col6a1*, *TenascinC* (*Tnc*), and proteoglycans in mutant Achilles tendon by real time PCR analysis. This experiment indicated that decorin (*Dcn*), which is a proteoglycan regulating collagen fiber formation, was down-regulated (Fig. S6). These data reveal that Mkx plays an important role in regulating the expression of type I collagen and its associate molecules in tendon cells.

Discussion

We investigated the in vivo functions of *Mkx*, the homeobox gene expressed in developing tendons, by analyzing the tendons of *Mkx* knockout mice. We examined two major tendons, Achilles and tail tendon, whose developmental origins are known to be different. Achilles tendon in the limbs is induced in mesenchyme directly and the tail tendon in the trunk is derived from syndetome (15, 29). As a result, cell density (Fig. 3*C*), collagen quantity (Fig. 4*A*) and type I collagen expressions (Fig. 4*B*) were reduced in both Achilles tendon and tail tendon of *Mkx* null mice. This indicates that Mkx may play a role in various tendons, regardless of the developmental origins, although such factors are unknown.

The bHLH transcription factor *Scx* is also known to be a positive regulator of tendon differentiation via its role in promoting type I collagen expression (17, 18). However, phenotypes of both null mutants are different. Although *Scx* null mutants exhibit a loss of segments or complete tendons (17), *Mkx* null mice have

reduced tendon mass without a decrease in the number of tendon cells. These data suggest that Scx is essential for the initiation of tendon differentiation, whereas Mkx plays a critical role in tendon maturation (Fig. 4*D*). Regardless of the high expression of *Scx* in *Mkx* null mice (Fig. S6), type I collagen gene expression is decreased (Fig. 4*C*), indicating the existence of other positive regulators of type I collagen that should be regulated by Mkx. Recent work indicates that Mkx functions as a transcriptional repressor by recruiting the Sin3A/histone deacetylase corepressor complex (30), therefore Mkx may act as a repressor for negative regulatory factors of type I collagen.

It has been reported that the *Tgfb2*, *Tgfb3* double knockout mice or *Tgfbr2* knockout mice show loss of most tendons, and TGF-β led to an early induction of a tendon master gene *Scx* expression (31). This indicates that TGF-β–Scx pathway regulates the initial differentiation of tendon. Here, we show that Mkx plays a critical role at the tendon maturation stage. It would be of interest to examine whether TGF-β may also be critical for late tendon differentiation via Mkx regulation.

To get more insight into the function of Mkx on the collagen network development, we examined a set of other tendon component genes' expressions and observed that decorin was also decreased in *Mkx* null mice tendons (Fig. S6). Reduced decorin, known to be a regulator of collagen assembly, expression may provide an explanation for the collagen fibril size reduction phenotype in *Mkx* null mice. Although we focused on tendon development, Mkx may also play a role in tendon homeostasis in adults. In this regard, it would be interesting to examine the potential function of Mkx in aging tendons.

These findings will serve as a basis for understanding molecular mechanisms of tendon differentiation and may provide a therapeutic target for tendon injuries and tendon related diseases, such as Ehlers-Danlos Syndrome.

Materials and Methods

Generation of Mkx Mutant Mice. All animal experiments were performed according to protocols approved by the Institutional Animal Care and Use Committee at the National Institute for Child Health and Development. A vector was constructed to replace the endogenous *Mkx* locus with the Venus gene and PGK-neo cassette by homologous recombination in ES cells (Fig. 1*A*). 5′ and 3′ sequences flanking the endogenous *Mkx* locus were amplified by PCR from a C57BL/6 genomic BAC clone (BACPAC Resource Center). These homology arms were cloned into a vector incorporating both a neomycin resistance cassette for positive selection and a diphtheria toxin (DT-A) gene for negative selection. The targeting vector was linearized and electroporated into TT2F ES cells. Recombinant ES clones were isolated after culture in medium containing G418 antibiotic and screened for proper integration by Southern blotting with the 5′probe, 3′probe and neo cassette sequence (Fig. S1 *A* and *B*). Two clones exhibited proper integration, which was validated through genomic sequencing, and were chosen for microinjection into eight-cell stage embryos. The resulting chimeric offspring were crossed to C57BL/6 mice and germ-line transmission was confirmed by Southern blotting (Fig. S1*C*) and PCR (Fig. 1*B*). The floxed PGK-neo cassette was removed by crossing with Meox-Cre transgenic mice (purchased from The Jackson Laboratory) (32) and Cre-mediated neo excision was analyzed by genomic PCR. PCR primer sequences for genotyping are shown in Table S2.

Whole-Mount Visualization of Fluorescent Signals and in Situ Hybridization. For whole-mount visualization of fluorescent signals, embryos were observed directly and tissues were skinned before observation. Whole-mount in situ hybridization for *Mkx* was performed as described previously (33). The details of *Mkx* probe synthesis for whole-mount in situ hybridization can be obtained on the "EMBRYS" web site (http://embrys.jp/embrys/html/MainMenu.html).

Histological Analysis and Immunohistochemistry. *Mkx* null mice and wild-type littermates were obtained from an intercross of $Mkx^{+/-}$ maintained on a C57BL/6 background. For histological analysis, patellar and tail tendons were harvested from embryos or adult mice and fixed with 4% paraformaldehyde in PBS at 4 °C overnight. Tissues were dehydrated, embedded in paraffin, and sectioned, and each section was stained with H&E or azocarmine-aniline blue (azan). For immunohistochemistry, tails from E16.5 embryos were dissected and fixed with 4% paraformaldehyde in PBS at 4 °C for 2 h. The tissues were embedded in O.C.T. compound (Sakura Finetek) and frozen rapidly in liquid nitrogen. Specimens were sectioned at 10 μm. Cryosections were air-dried and blocked with Blocking One (Nacalai Tesque) for 1 h. The sections were then incubated with anti-myosin heavy chain antibody (MF20; DSHB) at 4 °C overnight, rinsed, and incubated for 1 h with Alexa 594 (Molecular Probes). These experiments were performed with at least three independent samples to confirm reproducibility.

Tensile Testing. To evaluate the mechanical properties of the Achilles tendon, we used the entire tendon unit (from the myotendinous junction to the calcaneal tuberosity). A uniaxial materials testing system (Autograph AGS-G; Shimadzu Corp. Ltd.) was used to determine tensile properties with a 500 N load cell, as described previously (34) with some modifications. To facilitate gripping during testing, the proximal end of the Achilles tendon and foot of the mouse were fixed in custom-made clamps and the specimens were pulled at a constant strain rate of 0.5 mm/sec. All samples broke within the gauge length. The initial length and cross-sectional area of each specimen were measured using digital calipers and by microscopy of H&E stained sections, respectively. Force data were collected in Trapezium (Shimadzu Corp. Ltd.) software at a frequency of 50 Hz. For each specimen, a stress–strain curve was created from the load–displacement curve and Young's modulus was calculated from each stress–strain curve using the cross-sectional area.

Counting Cell Numbers of Tendon. The paraffin-sections or cryosections of tail or Achilles tendons from 3-month-old Mkx null or wild-type mice were prepared and stained with H&E or DAPI as described in Histological Analysis and Immunohistochemistry. The hematoxylin or DAPI stained nuclei were counted in each 50 μm × 50 μm area or tail tendon fiber bundle. At least eight areas or bundles were counted in three or four of Mkx null or wild-type mice.

Western Blot Analysis and Collagen Measurements. Total soluble protein was obtained from Achilles tendon and tail tendon by homogenization in RIPA buffer (50 mM Tris-HCl, 150 mM NaCl, 0.5% DOC, 0.1% SDS, 1% Nonidet P-40; pH 8.0) and used for Western blot analysis and collagen measurements. For Western blotting, total soluble protein was separated by SDS/PAGE followed by a semidry transfer to PVDF. Membranes were blocked for 30 min with Blocking One (Nacalai Tesque), incubated with anti-collagen I antibody (ab292; Abcam) or anti-β-actin antibody (A5316; SIGMA) at 4 °C overnight, rinsed, and then incubated for 1 h with HRP-conjugated anti-rabbit IgG (IgG) antibody (A6154; SIGMA) or HRP-conjugated anti-mouse IgG antibody (A2304; SIGMA). The blot was then developed with Chemi-Lumi One (Nacalai Tesque). Total soluble collagen measurements of homogenate in Achilles and tail tendons were performed using the Sircol Soluble Collagen Assay (Biocolor) according to the manufacturer's instructions. Total soluble protein was measured using the DC Protein Assay (Bio-Rad) and used the data for normalization. These experiments have been repeated at least three times to confirm reproducibility.

Electron Microscopy. Small pieces (approximately 1 mm^3) were excised from Achilles tendons of wild-type and *Mkx* null mice, and fixed with 4% paraformaldehyde and 2.5% glutaraldehyde in 0.1 M cacodylate buffer overnight. The samples were then washed in 0.1 M cacodylate buffer and rinsed with physiological saline. They were dehydrated through an ethanol series, embedded in epoxy resin, and cut into ultrathin (approximately 100 nm) sections. Sections were mounted on copper grids, contrasted with aqueous uranyl acetate and lead citrate and examined by transmission electron microscope (H-7100; Hitachi).

RNA Isolation, RT-PCR, and Quantitative Real-Time PCR. Total RNA was isolated from Achilles tendons, tail tendons and femoral muscles using ISOGEN (Nippongene), and reverse transcribed using Ready-To-Go You-Prime First-Strand Beads (GE Healthcare). RT-PCR was performed with Go-Taq polymerase (Promega). Quantitative real-time RT-PCR was performed with SYBR Green PCR Master Mix (Applied Biosystems). The expression of *Gapdh* was used as a control for mRNA expression. Gene expression changes were quantified using the delta-delta C_T method. This experiment was performed with three independent samples and confirmed reproducibility. Primer sequences for RT-PCR and real-time PCR are described in Table S2.

Statistical Analysis. The two-tailed independent Student's *t*-test was used to calculate all *P* values. Asterisks in figures indicate differences with statistical significance as follows: $*P < 0.05$, $**P < 0.01$, and $***P < 0.001$.

ACKNOWLEDGMENTS. We thank K. Sakuma, R. Higashiyama, A. Sawada, S. Ito, M. Horiuchi, J. Hasegawa, and T. Kotani for help with generation of *Mkx* mutant mice; M. Narasaki for technical assistance of ultrastructural analysis; and C. Shukunami, Y. Sugimoto, and Y. Nishizaki for beneficial advice. This project was supported by Grants from the Genome Network Project (Ministry of Education, Culture, Sports, Science and Technology) and partially from Solution-Oriented Research for Science and Technology (Japan Science and Technology Agency) and Grant ID05-24 from the National Institute of Biomedical Innovation.

1. Birk DE, Trelstad RL (1986) Extracellular compartments in tendon morphogenesis: Collagen fibril, bundle, and macroaggregate formation. *J Cell Biol* 103:231–240.
2. Sharma P, Maffulli N (2006) Biology of tendon injury: Healing, modeling and remodeling. *J Musculoskelet Neuronal Interact* 6:181–190.
3. Bi Y, et al. (2007) Identification of tendon stem/progenitor cells and the role of the extracellular matrix in their niche. *Nat Med* 13:1219–1227.
4. Kannus P (2000) Structure of the tendon connective tissue. *Scand J Med Sci Sports* 10: 312–320.
5. Yoon JH, Halper J (2005) Tendon proteoglycans: Biochemistry and function. *J Musculoskelet Neuronal Interact* 5:22–34.
6. Williams IF, McCullagh KG, Silver IA (1984) The distribution of types I and III collagen and fibronectin in the healing equine tendon. *Connect Tissue Res* 12:211–227.
7. Docheva D, Hunziker EB, Fässler R, Brandau O (2005) Tenomodulin is necessary for tenocyte proliferation and tendon maturation. *Mol Cell Biol* 25:699–705.
8. Benjamin M, Ralphs JR (2000) The cell and developmental biology of tendons and ligaments. *Int Rev Cytol* 196:85–130.
9. Kjaer M (2004) Role of extracellular matrix in adaptation of tendon and skeletal muscle to mechanical loading. *Physiol Rev* 84:649–698.
10. Danielson KG, et al. (1997) Targeted disruption of decorin leads to abnormal collagen fibril morphology and skin fragility. *J Cell Biol* 136:729–743.
11. Jepsen KJ, et al. (2002) A syndrome of joint laxity and impaired tendon integrity in lumican- and fibromodulin-deficient mice. *J Biol Chem* 277:35532–35540.
12. Ameye L, et al. (2002) Abnormal collagen fibrils in tendons of biglycan/fibromodulin-deficient mice lead to gait impairment, ectopic ossification, and osteoarthritis. *FASEB J* 16:673–680.
13. Chakravarti S, et al. (1998) Lumican regulates collagen fibril assembly: Skin fragility and corneal opacity in the absence of lumican. *J Cell Biol* 141:1277–1286.
14. Mao JR, Bristow J (2001) The Ehlers-Danlos syndrome: On beyond collagens. *J Clin Invest* 107:1063–1069.
15. Schweitzer R, et al. (2001) Analysis of the tendon cell fate using Scleraxis, a specific marker for tendons and ligaments. *Development* 128:3855–3866.
16. Cserjesi P, et al. (1995) Scleraxis: A basic helix-loop-helix protein that prefigures skeletal formation during mouse embryogenesis. *Development* 121:1099–1110.
17. Murchison ND, et al. (2007) Regulation of tendon differentiation by scleraxis distinguishes force-transmitting tendons from muscle-anchoring tendons. *Development* 134:2697–2708.
18. Léjard V, et al. (2007) Scleraxis and NFATc regulate the expression of the pro-alpha1(I) collagen gene in tendon fibroblasts. *J Biol Chem* 282:17665–17675.
19. Anderson DM, et al. (2006) Mohawk is a novel homeobox gene expressed in the developing mouse embryo. *Dev Dyn* 235:792–801.
20. Selleri L, et al. (2001) Requirement for Pbx1 in skeletal patterning and programming chondrocyte proliferation and differentiation. *Development* 128:3543–3557.
21. Brendolan A, et al. (2005) A Pbx1-dependent genetic and transcriptional network regulates spleen ontogeny. *Development* 132:3113–3126.
22. Moens CB, Selleri L (2006) Hox cofactors in vertebrate development. *Dev Biol* 291: 193–206.
23. van Tuyl M, et al. (2006) Iroquois genes influence proximo-distal morphogenesis during rat lung development. *Am J Physiol Lung Cell Mol Physiol* 290:L777–L789.
24. dilorio P, Alexa K, Choe SK, Etheridge L, Sagerström CG (2007) TALE-family homeodomain proteins regulate endodermal sonic hedgehog expression and pattern the anterior endoderm. *Dev Biol* 304:221–231.
25. Liu H, Liu W, Maltby KM, Lan Y, Jiang R (2006) Identification and developmental expression analysis of a novel homeobox gene closely linked to the mouse Twirler mutation. *Gene Expr Patterns* 6:632–636.
26. Takeuchi JK, Bruneau BG (2007) Irx1, a divergent Iroquois homeobox family transcription factor gene. *Gene Expr Patterns* 7:51–56.
27. Yokoyama S, et al. (2009) A systems approach reveals that the myogenesis genome network is regulated by the transcriptional repressor RP58. *Dev Cell* 17:836–848.
28. Nagai T, et al. (2002) A variant of yellow fluorescent protein with fast and efficient maturation for cell-biological applications. *Nat Biotechnol* 20:87–90.
29. Brent AE, Schweitzer R, Tabin CJ (2003) A somitic compartment of tendon progenitors. *Cell* 113:235–248.
30. Anderson DM, Beres BJ, Wilson-Rawls J, Rawls A (2009) The homeobox gene Mohawk represses transcription by recruiting the sin3A/HDAC co-repressor complex. *Dev Dyn* 238:572–580.
31. Pryce BA, et al. (2009) Recruitment and maintenance of tendon progenitors by TGFbeta signaling are essential for tendon formation. *Development* 136:1351–1361.
32. Tallquist MD, Soriano P (2000) Epiblast-restricted Cre expression in MORE mice: A tool to distinguish embryonic vs. extra-embryonic gene function. *Genesis* 26:113–115.
33. Yokoyama S, et al. (2008) Dynamic gene expression of Lin-28 during embryonic development in mouse and chicken. *Gene Expr Patterns* 8:155–160.
34. Gentleman E, et al. (2003) Mechanical characterization of collagen fibers and scaffolds for tissue engineering. *Biomaterials* 24:3805–3813.

The Journal of Clinical Pharmacology
http://jcp.sagepub.com/

Single- and Multiple-Dose Pharmacokinetics of the Selective Nicotinic Receptor Partial Agonist, Varenicline, in Healthy Japanese Adult Smokers

H. Kikkawa, N. Maruyama, Y. Fujimoto and T. Hasunuma

J Clin Pharmacol published online 15 June 2010
DOI: 10.1177/0091270010372388

The online version of this article can be found at:
http://jcp.sagepub.com/content/early/2010/06/15/0091270010372388

Published by:
SAGE
http://www.sagepublications.com

On behalf of:

American College of Clinical Pharmacology

J Clin Pharm OnlineFirst, published on June 15, 2010 as doi:10.1177/0091270010372388

Single- and Multiple-Dose Pharmacokinetics of the Selective Nicotinic Receptor Partial Agonist, Varenicline, in Healthy Japanese Adult Smokers

H. Kikkawa, PhD, N. Maruyama, PhD, Y. Fujimoto, MD, PhD, and T. Hasunuma, MD, PhD

Varenicline is a novel selective α4β2 nicotinic acetylcholine partial agonist developed for smoking cessation. Single- and multiple dose studies were conducted to investigate pharmacokinetics, safety, and tolerability of varenicline in healthy male Japanese smokers. The single-dose study was conducted as a double-blind, placebo-controlled, 4-way crossover study. Subjects received varenicline (0.25, 0.5, 1.0, 2.0 mg) or placebo at an interval of 2 weeks. The double-blind, placebo-controlled multiple-dose study was conducted as 2 cohorts, each consisting of 8 subjects randomized to varenicline tablets twice daily (0.5 or 1.0 mg) and 4 subjects randomized to placebo administered for 14 days. In both studies, varenicline was well tolerated at doses up to and including 2 mg daily. Dose-proportional increases in varenicline systemic exposure were observed following single and multiple dosing. Peak plasma concentrations generally occurred within 2 to 4 hours after dosing. Mean half-life estimates ranged from approximately 13 to 19 hours after single dosing and 24 to 28 hours after repeat dosing. Consistent with this, both 0.5 and 1.0 mg twice daily resulted, on average, in an approximate 3-fold increase in varenicline systemic exposure. These results showed that the single- and multiple-dose pharmacokinetics of varenicline in Japanese smokers were similar to those previously reported in Western smokers.

Keywords: *Varenicline; single dosing; multiple dosing; pharmacokinetics; smoking cessation*

Journal of Clinical Pharmacology, XXXX;XX:xxx-xxx

Tobacco smoking is widespread throughout the world and is one of the most prevalent modifiable risk factor for increased morbidity and mortality due to cancer, cardiovascular disease, and respiratory disease.[1] The World Health Organization projects that the number of deaths due to tobacco will grow to 10 million annually by 2030, and 70% of these deaths will be in developing countries.[2] Smoking is a major public health concern in Japan as well, and tobacco smoking accounted for an estimated 113 000 of 962 000 deaths in Japan in 2000.[3] Evidence suggests that smokers need excess medical care, especially inpatient care, and efforts to reduce tobacco exposure are imperative to improve the health care and economic burden on Japanese society.[4] Based on behavioral and pharmacological evidence, nicotine is the constituent in tobacco smoke that is thought to mediate dependence via α4β2 nicotinic acetylcholine receptor activation in the brain.[5,6]

Varenicline is a novel and selective nicotinic receptor partial agonist that binds specifically to the α4β2 receptor. Preclinical and clinical studies have demonstrated that varenicline is efficacious for smoking cessation by reducing the psychogenic reward associated with smoking and relieving nicotine craving and withdrawal symptoms.[7-11] Varenicline (Chantix/Champix) has been approved in more than 80 countries worldwide, including Japan in 2008, as an aid to smoking cessation. The pharmacokinetic (PK) and safety profiles of varenicline have been well characterized in the Western populations.[10-16] Varenicline exhibits linear kinetics when given as single or repeated doses up to 3 mg/day in smokers.[12,13] With single-dose oral administration of varenicline, smokers and nonsmokers tolerated up to 3 mg and 1 mg, respectively; nausea and vomiting were the dose-limiting factors.[12] With

From Pfizer Global R & D, Tokyo Laboratories, Pfizer Japan Inc, Tokyo, Japan (Dr Kikkawa, Dr Maruyama, Dr Fujimoto); and Research Center for Clinical Pharmacology, Kitasato University, Tokyo, Japan (Dr Hasunuma). Submitted for publication February 25, 2010; revised version accepted March 27, 2010. Address for correspondence: Hironori Kikkawa, Department of Clinical Pharmacology, Pfizer Global R & D, Tokyo Laboratories, Pfizer Japan Inc, 3-22-7, Yoyogi, Shibuya-ku, Tokyo 151-8589, Japan; e-mail: Hironori Kikkawa@japan.pfizer.com.
DOI:10.1177/0091270010372388

multiple-dose oral administration, varenicline 2 mg daily was the maximum tolerated dose in smokers. Results from a human balance study indicated that varenicline undergoes minimal metabolism with more than 90% of the administered dose excreted unchanged in urine, primarily via glomerular filtration with an elimination half-life of ~24 hours.[14,15] Oral bioavailability is unaffected by food or time-of-day dosing.[13] No marked ethnic-related differences in varenicline PK were to be expected, based on this information, between Japanese and Western populations. Two PK studies were conducted with the objective of assessing the safety, tolerability, and PK profiles of single and multiple oral doses of varenicline in healthy male Japanese smokers prior to the conduct of a confirmatory efficacy and safety trial in Japanese smokers.[9] The pharmacological effect of varenicline, as measured by the number of cigarettes smoked per day, was also investigated.

METHODS

Both single- and multiple-dose studies were conducted at the Bio-Iatric Center, Research Center for Clinical Pharmacology, Kitasato University (The Kitasato Institute, Tokyo, Japan) in compliance with the ethical principles originating from the revised Declaration of Helsinki (South Africa, 1996). Prior to the start of the studies, the protocol, case report form, subject information sheet, and consent form were reviewed and approved by the institutional review board of the Bio-Iatric Center. All subjects gave written informed consent to participate prior to undergoing any study procedures.

Subjects

Healthy Japanese male smokers aged 20 to 55 years were eligible if they were current cigarette smokers (≥10 cigarettes smoked per day, confirmed by positive urine cotinine test) with no period of abstinence of more than 3 months.

Single-dose study. Fourteen healthy volunteers were enrolled and 13 subjects completed the study. Subjects ranged in age from 20 to 34 years (mean 25.7), in height from 160.0 to 179.0 cm (mean 170.5), and in body weight from 52.3 to 75.4 kg (mean 61.9). All participants had normal renal function, as assessed by creatinine clearance values ranging from 84.8 to 130.8 mL/min (mean 106.8) using the Cockcroft-Gault formula.[17]

Multiple-dose study. Twenty-four healthy volunteers were enrolled and completed the study as planned. Subjects ranged in age from 20 to 29 years (mean 23.9), in height from 156.3 to 182.1 cm (mean 171.6), and in body weight from 51.3 to 78.9 kg (mean 62.4). All participants had normal renal function, as assessed by creatinine clearance values ranging from 86.4 to 147.9 mL/min (mean 118.7) using the Cockcroft-Gault formula.[17] There was no restriction on smoking during the study period in both the single- and multiple-dose studies. Alcohol, caffeine, and grapefruit juice were not permitted beginning 48 hours prior to the start of the study through the completion of each study. All subjects had been off prescription drug therapy, over-the-counter drugs, and health products (eg, vitamins, herbal remedies including herbal medicines) for at least 2 weeks prior to drug administration.

Study Design

Single-dose study. This was a randomized, double-blind, 4-way, incomplete block, crossover study. The 14 subjects were randomly allocated to active treatment or placebo in 5 sequences at a ratio of 3:1:1:1:1 (number of subjects in each sequence: 6:2:2:2:2) on the day of drug administration (day 1). Subjects received varenicline (0.25, 0.5, 1.0, or 2.0 mg) or placebo, from period I (0.25 mg) to period IV (2.0 mg), at an interval of approximately 2 weeks. Six of the 14 subjects received 0.25 to 2.0 mg sequentially, and other subjects received placebo in 1 of the 4 periods. Subjects proceeded to the next period after the investigator and study sponsor fully reviewed the subjects' health conditions and results of the interview and examinations and confirmed the subjects' safety.

Multiple-dose study. This study was a double-blind, placebo-controlled, multiple-dose, dose-escalation study, with doses administered twice a day for 14 days. Two cohorts, cohort 1 (0.5 mg or placebo twice daily) and cohort 2 (1.0 mg or placebo twice daily), were included. Subjects who were eligible to participate in this study after screening were admitted to the study site in the evening, 2 days prior to dosing for standard tests. On the dosing day, subjects were randomly allocated to receive the study drug or placebo in a 2:1 ratio. The investigator and study sponsor fully reviewed the safety and any adverse events (AEs) before dosing cohort 2 as described in

the single-dose study. Varenicline or placebo was administered in the morning and in the evening (every 12 hours).

Study Drug and Administration

In both dose studies, study medication (0.25, 0.5, and 1.0 mg varenicline and matched placebos) was supplied as immediate release tablets. The tablets were administered under fed conditions, and subjects were dosed within 5 minutes after a meal with 200 mL of water. In the single-dose study, subjects fasted for at least 8 hours prior to dosing. Subjects were dosed at approximately 8:00 A.M. immediately following breakfast, which was completely ingested over a 20-minute period. Subjects were required to stay up to 48 hours after dosing (day 3) for each study period. Subjects were kept under supervision of the principal investigator (subinvestigator) during the stay. They were discharged on day 3, after completion of all required assessments and approval by the investigator. In the multiple-dose study, subjects fasted for at least 2 hours prior to consuming breakfast or dinner and were dosed at approximately 8:00 A.M. or 8:00 P.M., respectively after completely ingesting the meal. Subjects were placed under the management of the principal investigator (subinvestigator) 2 days before the start of treatment until day 16. They were discharged on day 16 after completion of all required assessments and approval by the investigator. To standardize conditions, all subjects were required to refrain from lying down (except for vital sign and electrocardiogram [ECG] measurements), eating, and drinking beverages other than water during the first 4 hours after drug administration. Standardized meals consisting of breakfast, lunch, and dinner were served during the inpatient portion of the study. The daily nutritional composition was ~50% carbohydrates, ~35% fat, and ~15% protein.

Pharmacokinetic Sampling and Analysis

Plasma collection. In the single-dose study, blood sufficient to provide a minimum of 3 mL of plasma was collected in heparinized tubes for all 4 doses at the following times: 0 (immediately prior to the morning dosing), 0.5, 1, 2, 3, 4, 6, 8, 12, 24, 36, and 48 hours after drug administration; additional samples at 72 and 96 hours postdose were collected for the 1.0- and 2.0-mg dosing groups. In the multiple-dose study, blood samples were collected on day 1 at predose and nominally at 0.5, 1, 2, 4, 8, 12 (immediately prior to the evening dose), 12.5, 13, 14, 16, and 20 hours following the morning drug administration of varenicline. On day 14, blood samples were also collected at 24, 36, 48, 72, 96, and 144 hours following the last morning dose. Additional blood samples were drawn at predose (immediately prior to morning dosing) on days 2, 3, 4, 5, 8, and 11 and at 12 hours (immediately prior to the evening dosing) on days 2, 5, 8, and 11. Blood samples were centrifuged at 1700*g* for 10 minutes at approximately 4°C. The resultant plasma was stored in appropriately labeled screw-capped polypropylene tubes at −20°C or below within 1 hour of collection.

Urine collection. In the single-dose study, urine was collected immediately prior to dosing, over 0 to 6, 6 to 12, 12 to 24, and 24 to 48 hours post dose with 0.25 to 1.0 mg, and additionally collected at 48 to 72 and 72 to 96 hours post dose with 2.0 mg. In the multiple-dose study, urine was collected immediately prior to dosing and over 0 to 12 and 12 to 24 hours on day 1 and day 14. At the end of each urine collection period, the total volume was measured. The urine was then mixed thoroughly and a 5-mL aliquot from each collection period was retained, labeled, and frozen at −20°C until analysis. Aliquots necessary for urine electrolytes were also withdrawn from the same samples.

Assay method. Plasma and urine samples of subjects treated with varenicline were analyzed using a validated high performance liquid chromatography-atmospheric pressure ionization/tandem mass spectrometry assay following liquid–liquid extraction, as described previously.[16] The dynamic range of the assay using 1-mL aliquots was 0.100 to 50.0 ng/mL for plasma and 1.00 to 500 ng/mL for urine. A value of zero was assigned to plasma varenicline concentrations below the lower limit of quantification (0.100 ng/mL) for calculation of summary statistics.

Pharmacokinetic Evaluation

All PK parameters were estimated using standard noncompartmental methods (WinNonlin 3.1, Pharsight, Mountain View, California). For the single-dose study, maximum plasma concentrations (C_{max}) and the time of occurrence of C_{max} (T_{max}) were obtained directly from the experimental data. The area under plasma concentration–time curve from time zero to the last quantifiable concentration, C_{last} (AUC_{last}), was calculated using the linear/log trapezoidal method. The apparent elimination rate

constant (K_{el}) was estimated using linear least squares regression analysis of the plasma concentration–time data obtained during the terminal log-linear phase. The apparent terminal elimination half-life ($t_{1/2}$) was calculated as $\ln(2)/K_{el}$. The area under the plasma concentration–time curve extrapolated to infinity ($AUC_{0-\infty}$) was calculated as $AUC_{0-\infty} = AUC_{last} + C_{last}/K_{el}$. The percentage of $AUC_{0-\infty}$ extrapolation (AUC% extrapolated) was calculated as %AUC extrapolated = $(AUC_{0-\infty} - AUC_{last})/AUC_{0-\infty} \times 100$. Based on urinary excretion data, renal clearance (CL_R) was calculated as Ae_t/AUC_{last}, where Ae_t is the total amount of drug excreted unchanged in urine up to the last collection time point. For the multiple-dose study, C_{max} and T_{max} obtained on day 1 and day 14 and trough plasma concentration (C_{min}) were directly derived from the experimental data. The area under the plasma concentration–time curve from time zero to the end of the dosing interval (AUC_τ), where τ is the dosing interval equal to 12 hours for twice daily regimen, was estimated using the linear/log trapezoidal method. CL_R was calculated by dividing the amount of drug excreted unchanged in urine over the 12-hour dosing interval by the corresponding AUC_τ. The observed accumulation ratio (Rac_t) was determined as the ratio of AUC_τ on the last day of administration to AUC_τ on day 1 to assess changes in systemic exposure following repeated drug administration relative to single dosing.

Pharmacodynamic Evaluation

The baseline number of cigarettes smoked was recorded the days prior to dosing at the Clinic Research Center. The number of cigarettes smoked per day was recorded for each subject during the 14-day inpatient period of the multiple-dose study, and basic descriptive statistics (number of subjects, mean, median, standard deviation, minimum, and maximum) were calculated for each treatment group.

Safety Assessments

Safety and tolerability of varenicline were assessed in all subjects by clinical observation and spontaneous reporting of adverse events by subjects. Laboratory tests including urinalysis, hematology and clinical chemistry, blood pressure, pulse rate, body temperature, and 12-lead ECG measurements were performed at screening, during the inpatient period, and at follow-up visits.

Statistical Analysis

For both the single-dose and the multiple-dose studies, PK, pharmacodynamic, and safety data were summarized through appropriate data tabulations, descriptive statistics, and graphical presentations. No specific statistical hypothesis tests were planned. In the single-dose study, however, an exploratory assessment of dose proportionality was performed using the power model method described by Gough et al,[18] in which the logarithm of the PK parameter (C_{max}, AUC) is linearly related to the logarithm of dose. The slope and corresponding confidence interval were then estimated for each PK parameter.

RESULTS

Safety

Single-dose study. No deaths, serious adverse events, or discontinuation due to treatment-emergent AEs that were observed were reported during the study, including the lag period (7 days after dosing). One subject discontinued the study on day 15 in period I (0.25 mg) because of respiratory tract infection (investigator term: common cold) reported on day 10. Therefore, the study was conducted with 13 subjects from period II onward. Three treatment-emergent AEs were reported in 3 subjects (25%) in the 0.25-mg group, 3 events in 3 subjects (25%) in the 1.0-mg group, and 5 events in 2 subjects (18%) in the 2.0-mg group. All AEs were mild in severity. No AEs were reported in the 0.5-mg group and placebo groups. The treatment-related AEs were as follows: headache and retinal disorder (investigator term: soft retinal exudate) at 0.25 mg; diarrhea at 1 mg and abdominal pain, dyspepsia, and nausea in 1 subject; and abdominal pain and dyspepsia in 1 subject receiving 2.0 mg. With regard to the subject with the retinal disorder in the 0.25-mg group, a clear white spot was observed by funduscopy at 48 hours after dosing; the severity was mild and it was not observed at any other scheduled time points. Also, no clinically significant changes in laboratory tests, vital signs, and ECG were observed.

Multiple-dose study. No deaths, serious AEs, or discontinuations were reported. Adverse events were reported in 3 subjects (38%) receiving varenicline 0.5 mg twice daily, 4 (50%) receiving 1.0 mg twice daily, and 5 (63%) in the placebo group. All AEs were mild in severity, and all resolved during the study period. The most frequent AEs occurred in the

Table I Summary of Varenicline Pharmacokinetic Parameters After Single-Dose Oral Administration to Japanese Healthy Male Smokers

Pharmacokinetic Parameters, units		Varenicline Treatment			
		0.25 mg (n = 12)	0.5 mg (n = 11)	1.0 mg (n = 12)	2.0 mg (n = 11)
AUC_{last}, ng·h/mL	Arithmetic mean	23.0	46.6	101	220
	Standard deviation	4.3	5.7	11	45
	Geometric mean	22.7	46.2	100	217
	%CV	18.5	12.2	10.5	20.4
$AUC_{0-\infty}$, ng·h/mL	Arithmetic mean	26.2	50.0	104	226
	Standard deviation	3.9	5.9	11	47
	Geometric mean	25.9	49.7	104	222
	%CV	14.8	11.7	10.4	20.8
AUC % extrapolated	Median	10.8	6.0	3.2	2.2
	Range	7.1-22.1	3.2-10.0	1.9-3.7	0.9-4.0
C_{max}, ng/mL	Arithmetic mean	1.32	2.45	4.97	9.96
	Standard deviation	0.11	0.24	0.56	1.25
	Geometric mean	1.32	2.44	4.94	9.89
	%CV	8.5	9.9	11.2	12.5
T_{max}, h	Median	2.5	2.0	3.0	3.0
	Range	1.0-4.0	1.0-4.0	2.0-4.0	1.0-6.0
$t_{1/2}$, h	Arithmetic mean	13.1	14.5	18.4	19.3
	Standard deviation	2.1	2.4	3.2	2.2
CL_R, mL/min	Arithmetic mean	123	120	119	108
	Standard deviation	29	36	35	36
	Range	67.3-176	62.2-165	61.3-172	54.9-163

AUC, area under plasma concentration–time curve; AUC_{last}, area under plasma concentration–time curve from time zero to the last quantifiable concentration; $AUC_{0-\infty}$, area under the plasma concentration–time curve extrapolated to infinity; CL_R, renal clearance; C_{max}, maximum plasma concentration; CV, coefficient of variation; $t_{1/2}$, half-life.

digestive system (diarrhea, nausea, loose stools). Nausea was observed in 2 subjects in the 1.0-mg group. One subject experienced nausea 5 times (once on days 1, 2, 4, 6, and 8), and it was determined to be treatment related. In each instance, nausea occurred within 1 hour after dosing, was considered mild in severity, and resolved on the same day. The other subject experienced nausea once on day 9, but this occurrence was attributed to stress as a result of environmental changes and not related to treatment by the investigator. No clinically significant changes in laboratory tests, vital signs, and ECG were observed.

Pharmacokinetics

Single-dose study. The PK parameters and plasma concentration–time profiles in Japanese adult smokers are presented in Table I and Figure 1. The mean values of C_{max} after single doses of varenicline at 0.25, 0.5, 1.0, and 2.0 mg were 1.32, 2.45, 4.97, and 9.96 ng/mL, respectively. Over this dose range, plasma concentrations peaked at about 3 hours postdose. The means (ranges) of $t_{1/2}$ in each dose were 13.1 (9.8-15.9), 14.5 (11.8-19.2), 18.4 (12.5-22.3), and 19.3 (15.2-22.3) hours, respectively. The median percentage extrapolated areas under plasma concentration–time curve at 0.25, 0.5, 1.0, and 2.0 mg were 10.8%, 6.0%, 3.2%, and 2.2%, respectively. These values suggested that the elimination half-life of varenicline was accurately estimated in this study. Approximate dose-proportional increases in systemic exposure, as assessed by C_{max}, AUC_{last}, and $AUC_{0-\infty}$, were observed between 0.25 mg and 2.0 mg. Coefficients of variation (CV%) for C_{max}, AUC_{last}, and $AUC_{0-\infty}$ from 0.25 mg to 2.0 mg were 8.5% to 12.5%, 10.5% to 20.4%, and 10.4% to 20.8%, respectively, indicating that the observed variability in systemic exposure was generally low among subjects. Mean (± standard deviation) estimates of CL_R

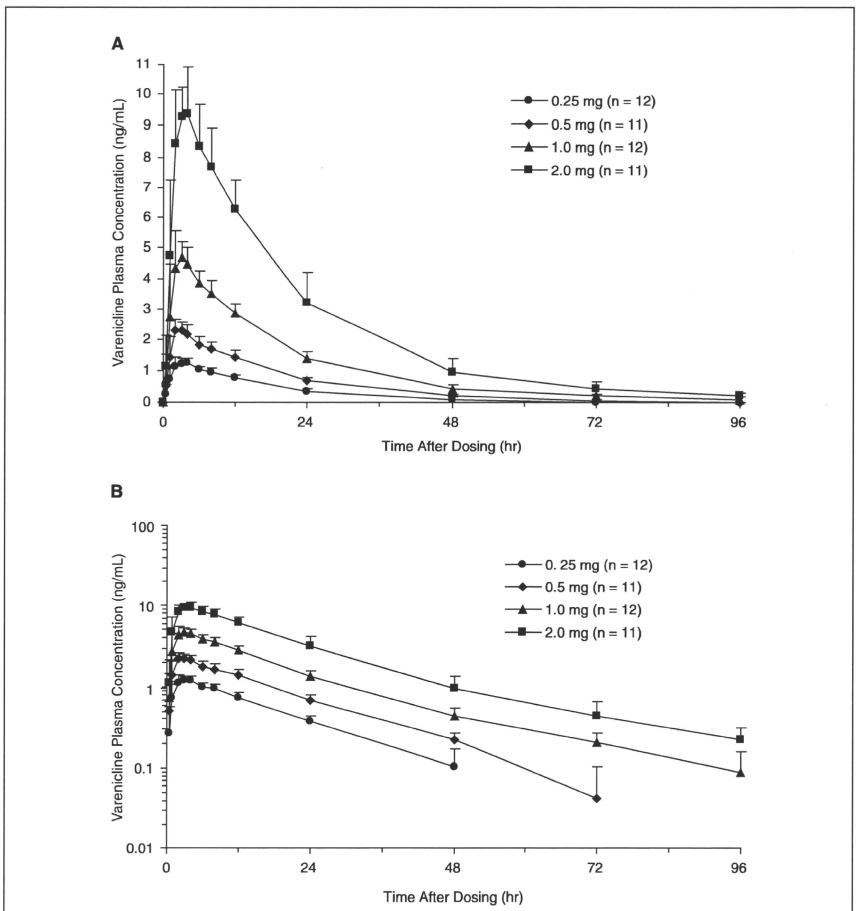

Figure 1. Mean (standard deviation) plasma concentration versus time plot of varenicline after single oral administration of different doses of varenicline under fed conditions in Japanese healthy male smokers (n =11 in 0.25-mg and 1.0-mg groups, n = 12 in 0.5-mg and 2.0-mg groups) on (A) a linear scale and (B) a semilogarithmic scale.

Table II Summary of Varenicline Pharmacokinetic Parameters After Multiple-Dose Oral Administration to Japanese Healthy Male Smokers

Pharmacokinetic Parameters, units		0.5 mg Twice Daily (n = 8)		1.0 mg Twice Daily (n = 8)	
		Day 1	Day 14	Day 1	Day 14
AUC_τ, ng·h/mL[a]	Arithmetic mean	21.8	58.5	42.7	116
	Standard deviation	3.0	10.4	6.1	29
	Geometric mean	21.6	57.8	42.3	114
	%CV	13.9	17.8	14.4	25.2
C_{max}, ng/mL[a]	Arithmetic mean	2.62	5.94	5.29	12.0
	Standard deviation	0.32	1.06	0.89	2.9
	Geometric mean	2.61	5.87	5.24	11.7
	%CV	12.3	17.8	16.8	15.5
T_{max}, h[a]	Median	3.0	4.0	2.5	3.0
	Range	1.0-4.0	2.0-4.0	1.0-4.0	2.0-4.0
$t_{1/2}$, h	Arithmetic mean	NA	28.0	NA	24.2
	Standard deviation	NA	4.5	NA	3.5
Rac_τ	Arithmetic mean	2.70		2.70	
	Standard deviation	0.40		0.32	
CL_R, mL/min	Arithmetic mean	79.0	83.7	99.3	90.5
	Standard deviation	14.8	14.9	23.7	20.0
	Range	63.6-102.6	73.9-141.8	60.9-105.9	46-112.7

AUC_τ, CL_R, renal clearance; C_{max}, maximum plasma concentration; CV, coefficient of variation; NA, not available; Rac_τ; accumulation ratio; T_{max}, time of occurrence of C_{max}; $t_{1/2}$, half-life; AUC_τ, The area under the plasma concentration-time curve from time zero to the end of the dosing interval, where τ is the 1st dosing interval equal to 12 hours.

a. Pharmacokinetic data for 0 to 12 hours after dosing (first dosing interval).

for varenicline ranged from 108 ± 36 mL/min to 123 ± 29 mL/min after single oral doses (Table I).

Although not an objective of the study, dose proportionality was investigated using the power model method based on dose-normalized geometric means for C_{max}, AUC_{last}, and $AUC_{0-\infty}$ across the entire dose range. Results of this analysis demonstrated that the value of the constant (β) of dose proportionality for C_{max} was estimated to be 0.99 (95% confidence interval [CI], 0.96-1.01), 1.09 (95% CI, 1.05-1.12) for AUC_{last}, and 1.04 (95% CI, 1.00-1.07) for $AUC_{0-\infty}$, indicating that varenicline PK was linear across the 0.25- to 2.0-mg range.

Multiple-dose study. The mean C_{max} and AUC_τ (area under the curve) on day 1 and day 14 increased in an approximately proportional manner with dose after multiple oral dosing of 0.5 or 1.0 mg varenicline twice daily (Table II, Figure 2). Based on the plasma trough concentration–time data, steady-state exposure to varenicline appeared to have been reached after 4 days of twice-daily dosing with both doses (Figure 3). The elimination half-life of varenicline estimated on day 14 was on average 28.0 hours (range, 19.2-34.5 hours) and 24.2 hours (range, 20.1-31.2 hours) in the 0.5- and 1.0-mg twice daily groups, respectively. The mean Rac_τ (standard deviation) was 2.7 (0.4) in the 0.5-mg group and 2.7 (0.3) in the 1.0-mg group. Median T_{max} (range) in the 0.5-mg group was 3.0 (1.0-4.0) hours and 4.0 (2.0-4.0) hours on days 1 and 14, respectively; in the 1.0-mg group, T_{max} was 2.5 (1.0-4.0) hours on both days 1 and 14. The elimination phase was adequately characterized in most subjects, and individual $t_{1/2}$ values were between 18 and 43 hours (mean $t_{1/2}$, 28.0 hours in 0.5 mg twice daily and 24.2 hours in 1.0 mg twice daily) after repeat dosing. Mean estimates of CL_r for varenicline were comparable between the initial dose on day 1 and after repeated administration on day 14 in both 0.5- and 1.0-mg twice daily dose regimens, ranging from 79.0 to 99.3 mL/min on day 1 and from 83.7 to 90.5 mL/min on day 14 (Table II).

Pharmacodynamics

The mean number of cigarettes smoked per day in the 1.0-mg twice daily group decreased markedly compared with placebo, whereas no clear difference was observed between 0.5 mg twice daily and placebo (Figure 4). The mean (standard deviation)

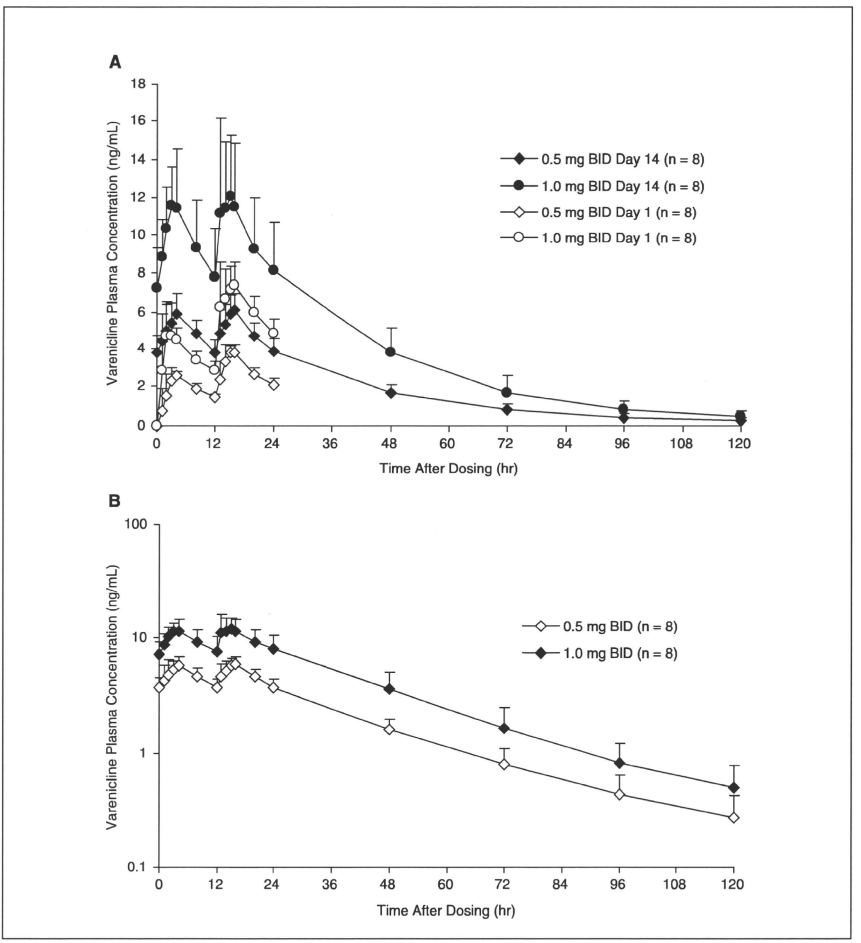

Figure 2. Mean (standard deviation) varenicline plasma concentration–time profiles following multiple oral doses of doses of 0.5 or 1 mg varenicline given twice daily to Japanese healthy male smokers on (A) both day 1 and day 14 on a linear scale and (B) day 14 on a semilogarithmic scale.

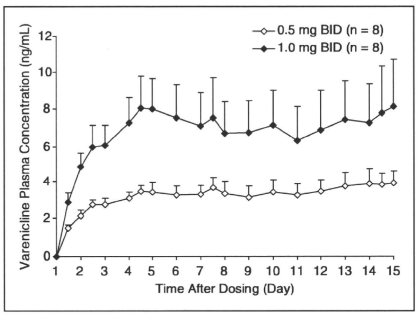

Figure 3. Mean (standard deviation) varenicline plasma trough concentration–time profiles following repeat oral administration of 0.5 or 1 mg varenicline given twice daily to Japanese healthy male smokers.

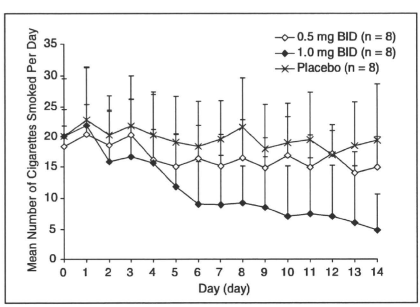

Figure 4. Mean number of cigarettes (± standard deviation) smoked per day following oral doses of varenicline (twice daily) or placebo to Japanese healthy male smokers. Dosing was initiated on day 1 and stopped on day 14.

number of cigarettes smoked on day 0 prior to the start of dosing was 20.1 (4.5), 18.4 (3.4), and 20.1 (9.5) in placebo, 0.5-mg twice daily, and 1.0-mg twice daily groups, respectively. At the end of the 14-day study, the mean (standard deviation) number of cigarettes was 19.4 (9.3), 14.9 (5.1), and 4.9 (5.7) in the placebo, 0.5-mg twice daily, and 1.0-mg twice daily groups, respectively. Although subjects were allowed to freely smoke their usual cigarette brand during the conduction of the study and specifically were asked not to change their smoking habits, it was noted that an increasing number of subjects receiving varenicline 1.0 mg twice daily did not smoke any cigarettes on a given day from day 5 onward. In fact, half of the male smokers (4/8) in this dose group stopped smoking by day 14, and 2 of these individuals were able to maintain their cessation for at least a week.

DISCUSSION

Orally administered varenicline exhibited a favorable safety profile in healthy Japanese male smokers, with single and multiple doses being well tolerated up to and including 2.0 mg daily. Overall, there was no apparent effect of varenicline on clinical laboratory assessments, vital signs, QTc, or ECG morphology. One subject in the 0.25-mg group experienced a transient, mild retinal disorder at 48 hours after dosing. There was no abnormality in vision or any other subjective and objective symptoms. Also, this AE did not recur despite increasing the dose in the subsequent periods. It was considered that the cause of the white spot in the fundus was a spontaneous infarction or spasm of the retinal artery resulting in ischemia or necrosis of the tissue. If the retinal vessel change had been caused by study drug or systemic disorders, this would have resulted in multiple white spots and other blood vessel lesions such as vasospasm, vaso-occlusion, or crossing phenomenon. Although the possibility of an artifact could not be completely rejected, this AE was considered to be a retinal soft exudate as only a single white spot was found and no other vessel lesions were observed. No such AE was reported in the multiple-dose study. In both the single- and multiple-dose studies, nausea was the most frequently reported AE. Nausea was generally transient, occurring within 1 hour of dosing, and considered mild in severity. This is consistent with the findings in Western studies.[13]

Following single-dose administration, dose-proportional increases in C_{max} and $AUC_{0-\infty}$ values were observed across the dose range of 0.25 to 2.0 mg. Maximum plasma concentration was typically achieved within 2 to 4 hours after dosing. When varenicline was administered twice daily, systemic exposure at steady state, as assessed by C_{max} and AUC_{τ}, increased about 3-fold over the 12-hour dosing interval. The extent of the observed increases in systemic exposure at steady state was consistent with $t_{1/2}$ and well predicted from single dosing ($AUC_{\tau}/AUC_{(0-\infty)}$ ~ 1). Additionally, when comparing steady-state

exposure of the evening dose to that of the morning dose, both the ratios of $AUC_{(12-24)}/AUC_{(0-12)}$ and C_{max} (evening dose)/C_{max} (morning dose) were near 1 following 0.5- and 1.0-mg twice daily dose regimens, suggesting a lack of diurnal variation in the varenicline steady-state PK. Estimates of renal clearance were similar across the range of single and multiple doses, indicating that the elimination process of varenicline was not altered upon repeat dosing.

Comparison of the PK properties of varenicline in these healthy Japanese smokers with those obtained in healthy Western smokers generally showed good agreement.[13,15] As reported by Faessel et al[13], mean (standard deviation) C_{max} and AUC_{τ} values following oral administration of varenicline 1 mg twice daily were 4.08 ng/mL (0.82) and 39.3 ng·h/mL (7.3) after single dosing and 10.2 ng/mL (1.0) and 105 ng·h/mL (16) after repeat dosing. This is expected as varenicline is predominantly excreted unchanged via the kidney and not oxidatively metabolized.[14] Mean plasma peak concentrations appeared slightly (<20%) increased in Japanese subjects. Because varenicline distributes readily throughout the body and the Japanese subjects weighed less on average than those in the Western populations, the observed difference in C_{max} may potentially be related to an effect of body size, as described in a population PK analysis.[19]

A decrease in the number of cigarettes smoked per day in male Japanese smokers who had no intention to quit smoking was observed following administration of varenicline 1 mg twice daily. The decreasing trend was consistent with the attainment of steady-state conditions of varenicline. It was noted that the subjects who stopped smoking at the 1-mg twice daily dose level had slightly higher steady-state systemic exposure than others. These observed trends were comparable with those previously observed in the Western smoking population.[13]

In conclusion, varenicline was well tolerated in Japanese adult smokers across the range of 0.25 to 2 mg daily dose. The PK findings demonstrated that the single- and multiple-dose PK properties of varenicline in Japanese smokers were comparable to those in Western smokers.

We thank Eriko Miyawaki, the clinical research associate at Pfizer Japan Inc, and the staff at the Bio-Iatric Center, Research Center for Clinical Pharmacology, Kitasato University. We thank Kevin Rohrbacher for coordinating the PK sample analysis with Alta Lab (El Dorado Hills, Calif). We are especially grateful to Dr. Hélène M. Faessel and Taro Ishibashi for their valuable comments on the study and manuscript.

Financial disclosure: The study was funded by Pfizer Inc. Drs Kikkawa, Maruyama, and Fujimoto are employees of Pfizer Japan Inc (Tokyo, Japan). Dr. Hasunuma was the primary study investigator and has received research contracts from Pfizer Japan Inc.

REFERENCES

1. Ezzati M, Lopez AD. Estimates of global mortality attributable to smoking in 2000. *Lancet.* 2003;362:847-852.

2. Quantifying selected major risks to health. World Health Report 2002. Geneva, Switzerland: World Health Organization, 2002; http://www.who.int/whr/2002/en/whr02_ch4.pdf. Accessed April 30, 2009.

3. Peto R, Lopez AD, Boreham J, Thun M. Mortality from smoking in developed countries 1950–2000. 2006 revision. http://www.ctsu.ox.ac.uk/~tobacco/. Accessed April 30, 2009.

4. Izumi Y, Tsuji I, Ohkubo T, et al. Impact of smoking habit on medical care use and its costs: a prospective observation of National Health Insurance beneficiaries in Japan. *Int J Epidemiol.* 2001;30:616-621.

5. Tapper AR, McKinney SL, Nashmi R, et al. Nicotine activation of alpha4* receptors: sufficient for reward, tolerance, and sensitization. *Science.* 2004;306:1029-1032.

6. Picciotto MR, Zoli M, Rimondini R, et al. Acetylcholine receptors containing the beta2 subunit are involved in the reinforcing properties of nicotine. *Nature.* 1998;391:173-177.

7. Rollema H, Chambers LK, Coe JW, et al. Pharmacological profile of the α4β2 nicotinic acetylcholine receptor partial agonist varenicline, an effective smoking cessation aid. *Neuropharmacology.* 2007;52:985-994.

8. Coe JW, Brooks PR, Vetelino MG, et al. Varenicline: an alpha-4beta2 nicotinic receptor partial agonist for smoking cessation. *J Med Chem.* 2005;48:3474-3477.

9. Nakamura M, Oshima A, Fujimoto Y, Maruyama N, Ishibashi T, Reeves KR. Efficacy and tolerability of varenicline, an alpha-4beta2 nicotinic acetylcholine receptor partial agonist, in a 12-week, randomized, placebo-controlled, dose-response study with 40-week follow-up for smoking cessation in Japanese smokers. *Clin Ther.* 2007;29:1040-1056.

10. Gonzales D, Rennard SI, Nides M, et al. Varenicline, an alpha4beta2 nicotinic acetylcholine receptor partial agonist, vs sustained-release bupropion and placebo for smoking cessation: a randomized controlled trial. *JAMA.* 2006;296:47-55.

11. Jorenby DE, Hays JT, Rigotti NA, et al. Efficacy of varenicline, an alpha4beta2 nicotinic acetylcholine receptor partial agonist, vs placebo or sustained-release bupropion for smoking cessation: a randomized controlled trial. *JAMA.* 2006;296:56-63.

12. Faessel HM, Smith BJ, Gibbs MA, et al. Single-dose pharmacokinetics of varenicline, a selective nicotinic receptor partial agonist, in healthy smokers and nonsmokers. *J Clin Pharmacol.* 2006;46:991-998.

13. Faessel HM, Gibbs MA, Clark DJ, Morse TA, Burstein AH. Multiple dose pharmacokinetics and pharmacodynamics of the nicotinic receptor partial agonist, varenicline, in healthy smokers. *J Clin Pharmacol.* 2006;46:1439-1448.